The Reduction Pathway of End-on Coordinated Dinitrogen. II. Electronic Structure and Reactivity of Mo/W−N_2, −NNH, and −NNH_2 Complexes

Nicolai Lehnert and Felix Tuczek*

Institut für Anorganische Chemie und Analytische Chemie der Universität Mainz, Staudinger Weg 9, D-55099 Mainz, Germany

Received August 7, 1998

DFT calculations (B3LYP/LanL2DZ) of simplified models of $[Mo(N_2)_2(dppe)_2]$ and the two protonated derivatives $[MoF(NNH)(dppe)_2]$ and $[MoF(NNH_2)(dppe)_2]^+$ (dppe = 1,2-bis(diphenylphosphino)ethane) provide quantitative insight into the reduction and protonation of dinitrogen bound end-on terminally to transition metals. This "asymmetric" reduction pathway is characterized by a stepwise increase of covalency and a concomitant charge donation from the metal center during each protonation reaction. The major part of metal-to-ligand charge transfer occurs after the first protonation leading to coordinated diazenido(−). In contrast, addition of the second proton is accompanied by a minor change of covalency leading to a NNH_2 species which is neutral and hence corresponds to coordinated isodiazene. UV−vis data of Mo and corresponding W complexes support the calculated energy level schemes. Moreover, calculated vibrational frequencies and force constants show good agreement with experimental values determined in Part I of this series (Lehnert, N.; Tuczek, F. *Inorg. Chem.* **1999**, 38, 1659−1670). The implications of the electronic structure description obtained for the above model complexes with respect to the reduction and protonation of dinitrogen in small-molecule systems and nitrogenase are discussed.

Introduction

The elucidation of the mechanism of biological nitrogen fixation and the realization of a corresponding catalytic cycle based on synthetic dinitrogen systems represent major challenges to bioinorganic and coordination chemistry.[1] Although principally different, these two goals have always been considered as related based on the assumption that the understanding of the biological process on a molecular level would open a way to synthetic nitrogen fixation at room temperature and ambient pressure, or, *vice versa*, that from a catalytic system *in vitro* something could be learnt regarding the detailed functioning of the enzyme. With respect to the latter approach, the requirement of "mild conditions" has been stressed repeatedly.[2] In particular, this implies that strongly negative reduction potentials should be avoided.

Unfortunately, the structure determination of the iron/molybdenum cofactor (FeMoCo)[3] of the enzyme nitrogenase has afforded no information as to where and in which geometry N_2 is bound and reduced.[4] Nevertheless, from the many possible coordination modes and sites of dinitrogen at the cofactor, two binding geometries can be considered as most probable based upon information from small-molecule model complexes,[5] structural considerations and molecular orbital calculations,[6] i.e. the *end-on terminal* and the *edge-on* coordination of N_2 to an Fe_4-face of the FeMoCo. Importantly, these two bonding modes also entail *two different reduction pathways*, both of which can be reproduced with synthetic compounds. It is therefore of interest to analyze in detail and compare these pathways both of which represent probable scenarios for the biological process using relevant small-molecule systems as models for the various stages of N_2 reduction in the enzyme. Alternatively, this will provide insight concerning the influence of the different bonding modes of dinitrogen on the *activation toward protonation* and the *stabilization of protonated intermediates* which is also highly relevant to synthetic N_2 fixation. In this respect, a further point of interest is the dependence of reactivity on the central metal and the coligands. It has been stressed that a full understanding of all of these factors is still lacking to date.[7]

The *end-on terminal* coordination of N_2 above an Fe_4-face of the FeMoCo follows as the most favourable configuration from comparative calculations of Hoffmann et al.[8] considering the fact that N_2 cannot replace one of the bridging S^{2-} groups. This bonding mode has also been put forward by extended-Hückel calculations of Plass.[9] As a consequence of the primary end-on bonding mode of dinitrogen, protonation to NH_3 would proceed initially via intermediates NNH_x which are well known from simple mononuclear Mo/W−phosphine complexes.[10] In the small-molecule systems, the asymmetric coordination of N_2 causes a negative partial charge at the β-nitrogen. Successive

* Corresponding author.

(1) (a) Tuczek, F.; Lehnert, N. *Angew. Chem.* **1998**, *110*, 2780. (b) Rawls, R. L. *Chem. Eng. News* **1998**, *76*, 29.
(2) Sellmann, D.; Sutter, J. *Acc. Chem. Res.* **1997**, *30*, 460.
(3) (a) Kim, J.; Rees, D. C. *Science* **1992**, *257*, 1677. (b) Kim, J.; Rees, D. C. *Nature* **1992**, *360*, 553. (c) Chan, M. K.; Kim, J., Rees, D. C. *Science* **1993**, *260*, 792. (d) Bolin, J. T.; Ronco, A. E., Morgan, T. V.; Mortenson, L. E.; Xuong, N. H. *Proc. Natl. Acad. Sci. U.S.A.* **1993**, *90*, 1078. (e) Chen, J.; Christiansen, J.; Campobasso, N.; Bolin, J. T.; Tittsworth, R. C.; Hales, B. J.; Rehr, J. J.; Cramer, S. P. *Angew. Chem.* **1993**, *105*, 1661.
(4) (a) Orme-Johnson, W. H. *Science* **1992**, *257*, 1639. (b) *Molybdenum Enzymes, Cofactors and Model Systems*; Stiefel, E. I., Coucouvanis, D., Newton, W. E., Eds.; American Chemical Society: Washington, DC, 1993. (c) Howard, J. B.; Rees, D. C. *Chem. Rev.* **1996**, *96*, 2965. (d) Burgess, B. K.; Lowe, D. J. *Chem. Rev.* **1996**, *96*, 2983.
(5) (a) Hidai, M.; Mizobe, Y. *Chem. Rev.* **1995**, *95*, 1115. (b) Chatt, J.; Dilworth, J. R.; Richards, R. L. *Chem. Rev.* **1978**, *78*, 589. (c) Henderson, R. A.; Leigh, G. J.; Pickett, C. J. *Adv. Inorg. Chem. Radiochem.* **1983**, *27*, 197.
(6) Dance, I. *J. Biol. Inorg. Chem.* **1996**, *1*, 581.
(7) Leigh, G. J. *Acc. Chem. Res.* **1992**, *25*, 177.
(8) Deng, H.; Hoffmann, R. *Angew. Chem.* **1993**, *105*, 1125.
(9) Plass, W. *J. Mol. Struct. (THEOCHEM)* **1994**, *315*, 53.

10.1021/ic9809409 CCC: $18.00
Published on Web 04/01/1999

protonation at this atom leads via the "diazenido(−)" (NNH), "hydrazido(2−)" (NNH_2) and "hydrazidium" (NNH_3^+) intermediates to the splitting of the N−N bond, generation of NH_3 and formation of the nitride complex which again can be protonated to give one more molecule of NH_3 (eq 1).[5,7]

$$M-N_2 \xrightarrow[H^+]{e^-} M-NNH \xrightarrow[H^+]{e^-} M-NNH_2 \xrightarrow[H^+]{e^-} M-NNH_3 \xrightarrow[-NH_3]{} M-N \xrightarrow[3H^+]{3e^-} M-NH_3 \quad (1)$$

The relevance of this chemistry to nitrogenase has been stressed many years ago by Lowe and Thorneley.[11] It should be noted that the actual protonation sequence involving the Mo and W systems is more complicated than described by eq 1.[5] Nevertheless, most of the intermediates involved in this scheme have been structurally characterized. In the preceding paper, the vibrational properties of the first three species have been investigated in detail. Although the parent dinitrogen systems exhibit only slightly enlarged N−N bond lengths and N−N stretching frequencies of about 2000 cm^{-1} and therefore contain only moderately activated N_2, the yields of ammonia in this "asymmetric" pathway are high. Without adding electrons, Mo(0)/W(0) are oxidized to Mo(VI)/W(VI) in the course of these reactions. With small yields of NH_3, however, the process also can be carried through electrochemically in a cyclic way.[12]

Alternatively, dinitrogen is bound in an *edge-on* coordination to an Fe_4-face of the FeMoCo. This initial bonding geometry has been advanced by Dance[6,13] on the basis of DFT calculations. Binuclear *side-on* (or *edge-on*) *dinitrogen bridged* compounds, which are primarily known from low-valent early transition metals,[15] may be considered as relevant low-molecular weight models of this coordination mode of nitrogenase. They contain such highly activated dinitrogen that protonation to hydrazine (presumably via a diazene intermediate) occurs without difficulty.[5a] The reduction of C_2H_2 in D_2O to *cis*-$C_2H_2D_2$[14] indicates that such a "symmetric" pathway is in fact also possible for nitrogenase. Symmetrically bound N_2 (i.e. with both N atoms) is also contained in some *linear end-on N₂-bridged* complexes which can be protonated. As evidenced by large N−N distances and correspondingly low dinitrogen stretching frequencies, the N_2 ligands are also highly activated in these compounds.[7] In general, such a high degree of activation is induced by metals with d-electrons of high energy and strong reducing capacities such as low-valent early transition metals (Ti and V group) and/or strongly reducing ligand systems. In contrast to the side-on systems, however, this class of compounds is of no direct relevance to nitrogenase as FeMoCo cannot bind N_2 in an end-on bridging way. Nevertheless, members of this class also follow a symmetric reduction pathway since protonation and reduction first lead to coordinated diazene (HNNH) and, after further addition of two protons and electrons, to hydrazine (H_2NNH_2).[7] The binuclear *trans*-μ-1,2-diazene complexes of Sellmann et al.[16] which we have studied in detail in a previous publication[17] serve as models for the first stage of reduction along this pathway. Alternative symmetric reduction schemes involve side-on coordinated diazene and hydrazine species[18] and the splitting of the N−N bond upon coordination of N_2.[19]

This study considers the first steps of the asymmetric path based on Mo−NNH_x ($x = 0-2$) systems. In the preceding paper in this issue, the vibrational properties of the Mo−N_2 complex $[Mo(N_2)_2(dppe)_2]$ (**Ia**) and the analogous W−NNH_x ($x = 0-2$) systems $[W(N_2)_2(dppe)_2]$ (**Ib**), $[WF(NNH)(dppe)_2]$ (**IIb**), and $[WF(NNH_2)(dppe)_2]^+$ (**IIIb**; dppe = 1,2-bis(diphenylphosphino)ethane) have been studied in detail. In our spectroscopic studies we had decided to focus on the tungsten compounds due to their higher photochemical stability in the Raman experiments, whereas the calculations presented here are mainly performed on molybdenum systems. Specifically, we determine the MO diagrams and charges of the model complexes $[Mo(N_2)_2(PH_3)_4]$ (**Ĭa**), $[MoF(NNH)(PH_3)_4]$ (**ĨIa**), and $[MoF(NNH_2)(PH_3)_4]^+$ (**ĨIIa**). In combination with orbital compositions and calculated charges, the obtained MO schemes allow an electronic-structural analysis of the asymmetric reduction mode of N_2 and define the corresponding orbital pathway. Based on these results and on a qualitative discussion of the symmetric pathway, the relevant features of both pathways are compared.

Quantum-chemical studies on the mentioned systems have been carried out before.[20] In a classic study, Hoffmann et al. have treated various transition-metal complexes containing N_2 and NNR_x ligands with extended-Hückel theory[21] and established the qualitative bonding schemes of these ligands with transition metal centers. In order to obtain a quantitative description of the above mentioned systems, we apply density functional theory using the B3LYP functional and compare spectroscopic properties derived by this method with experi-

(10) (a) Chatt, J.; Heath, G. A.; Richards, R. L. *J. Chem. Soc., Chem. Commun.* **1972**, 1010. (b) Chatt, J.; Heath, G. A.; Richards, R. L. *J. Chem. Soc., Dalton Trans.* **1974**, 2074. (c) Heath, G. A.; Mason, R.; Thomas, K. M. *J. Am. Chem. Soc.* **1974**, *96*, 260. (d) Chatt, J.; Pearman, A. J.; Richards, R. L. *J. Chem. Soc., Dalton Trans.* **1976**, 1520. (e) Chatt, J.; Pearman, A. J.; Richards, R. L. *J. Chem. Soc., Dalton Trans.* **1977**, 1852. (f) Chatt, J.; Pearman, A. J.; Richards, R. L. *J. Chem. Soc., Dalton Trans.* **1977**, 2139. (g) Chatt, J.; Pearman, A. J.; Richards, R. L. *J. Chem. Soc., Dalton Trans.* **1978**, 1766. (h) Takahashi, T.; Mizobe, Y.; Sato, M.; Uchida, Y.; Hidai, M. *J. Am. Chem. Soc.* **1980**, *102*, 7461. (i) Chatt, J.; Fakley, M. E.; Hitchcock, P. B.; Richards, R. L.; Luong-Thi, N. T. *J. Chem. Soc., Dalton Trans.* **1982**, 345. (j) George, T. A.; Tisdale, R. C. *J. Am. Chem. Soc.* **1985**, *107*, 5157. (k) Abu Bakar, M.; Hughes, D. L.; Hussain, W.; Leigh, G. J.; Macdonald, C. J.; Mohd.-Ali, H. *J. Chem. Soc., Dalton Trans.* **1988**, 2545. (l) Barclay, J. E.; Hills, A.; Hughes, D. L.; Leigh, G. J.; Macdonald, C. J.; Abu Bakar, M.; Mohd.-Ali, H. *J. Chem. Soc., Dalton Trans.* **1990**, 2503. (m) Galindo, A.; Hills, A.; Hughes, D. L.; Richards, R. L.; Hughes, M.; Mason, J. *J. Chem. Soc., Dalton Trans.* **1990**, 283. (n) George, T. A.; Ma, L.; Shailh, S. N.; Tisdale, R. C.; Zubieta, J. *Inorg. Chem.* **1990**, *29*, 4789. (o) George, T. A.; Kaul, B. B.; Chen, Q.; Zubieta, J. *Inorg. Chem.* **1993**, *32*, 1706. (p) Jimenez-Tenorio, M.; Puerta, M. C.; Valerga, P.; Hughes, D. L. *J. Chem. Soc., Dalton Trans.* **1994**, 2431.
(11) Thorneley, R. N. F.; Lowe, D. J. In *Molybdenum Enzymes*; Spiro, T. G., Ed.; John Wiley, New York, 1985.
(12) Pickett, C. J.; Talarmin, J. *Nature* **1985**, *317*, 652.
(13) Dance, I. G. *Aust. J. Chem.* **1994**, *47*, 979.
(14) Burgess, B. K. In *Molybdenum Enzymes*; Spiro, T. G., Ed.; John Wiley: New York 1985 and references therein.
(15) (a) Duchateau, R.; Gambarotta, S.; Beydoun, N.; Bensimon, C. *J. Am. Chem. Soc.* **1991**, *113*, 8986. (b) Fryzuk, M. D.; Haddad, T. S.; Mylvaganam, M.; McConville, D. H.; Rettig, S. J. *J. Am. Chem. Soc.* **1993**, *115*, 2782. (c) Cohen, J. D.; Mylvaganam, M.; Fryzuk, M. D.; Loehr, T. M. *J. Am. Chem. Soc.* **1994**, *116*, 9529. (d) Fryzuk, M. D.; Love, J. B.; Rettig, S. J.; Young, V. G. *Science* **1997**, *275*, 1445. (e) Cohen, J. D.; Fryzuk, M. D.; Loehr, T. M.; Mylvaganam, M.; Rettig, S. J. *Inorg. Chem.* **1998**, *37*, 112.
(16) (a) Sellmann, D.; Böhlen, E.; Waeber, M.; Huttner, G.; Zsolnai, L. *Angew. Chem.* **1985**, *97*, 984. (b) Sellmann, D.; Soglowek, W.; Knoch, F.; Moll, M. *Angew. Chem.* **1989**, *101*, 1244. (c) Sellmann, D.; Friedrich, H.; Knoch, F.; Moll, M. *Z. Naturforsch.* **1994**, *48b*, 76.
(17) (a) Lehnert, N.; Wiesler, B. E.; Tuczek, F.; Hennige, A.; Sellmann, D. *J. Am. Chem. Soc.* **1997**, *119*, 8869. (b) Lehnert, N.; Wiesler, B. E.; Tuczek, F.; Hennige, A.; Sellmann, D. *J. Am. Chem. Soc.* **1997**, *119*, 8879.
(18) Schrock, R. R.; Glassman, T. E.; Vale, M. G.; Kol, M. *J. Am. Chem. Soc.* **1993**, *115*, 1760 and references therein.
(19) (a) Laplaza, C. E.; Cummins, C. C. *Science* **1995**, *268*, 861. (b) Laplaza, C. E.; Johnson, A. R.; Cummins, C. C. *J. Am. Chem. Soc.* **1996**, *118*, 709.
(20) Pelikán, P.; Boča, R. *Coord. Chem. Rev.* **1984**, *55*, 55.
(21) DuBois, D. L.; Hoffmann, R. *Nouv. J. Chim.* **1977**, *1*, 479.

Table 1. Comparison of Experimental and Calculated Structures Applied on the Model Systems **Ĩa**−**IĨIa**

complex	data[a] from	bond lengths[b] M−P[c]	M−N	N−N	M−X	N−H	angle N−N−H	literature
$[Mo(N_2)_2(PH_3)_4]$ (**Ĩa**)	X-ray[d]	2.45	2.014	1.118				30a
	Opt	2.510	2.014	1.164				−
$[MoF(NNH)(PH_3)_4]$ (**IĨIa**)	X-ray	not known						−
	Opt[e]	2.54	1.826	1.276	2.07	1.038	114	−
$[MoF(NNH_2)(PH_3)_4]^+$ (**IĨIIa**)	X-ray[f]	2.54	1.763	1.332	1.99	1.09	125	30b
	Opt	2.594	1.786	1.331	1.99	1.01	120	−

[a] Opt: optimized structure. [b] In Å; all P−H bond lengths are set to 1.420 Å for calculation. [c] Data are averaged when necessary. [d] Used for calculation. [e] For calculation, the N−H bond length was set to 1.05 Å and the corresponding N−N−H angle to 115°. [f] Used for calculation; the N−H bond length and the N−N−H angle in the original structure of **IIIa** are distorted and therefore idealized.

mental data. In particular, the calculated orbital energies are used to interpret the UV−vis CT spectra of the Mo and W complexes. For **Ĩa**−**IĨIa** and the W−N_2 complex (**Ĩb**), vibrational frequencies and force constants have been calculated as well. The obtained values show good agreement with experiment and thus support our bonding descriptions.

Experimental and Computational Procedures

Sample Preparation and UV−Vis Spectroscopy. The dinitrogen complexes of molybdenum and tungsten with the dppe ligand as well as the derived protonated species of tungsten were prepared following literature procedures.[22] Purity was checked by elemental analysis. UV−vis spectra were measured with a Bruins Omega-10 spectrometer.

DFT Calculations. Spin-restricted DFT calculations using Becke's three parameter hybrid functional with the correlation functional of Lee, Yang and Parr (B3LYP[23]) were performed for the singlet ground state of simplified models **Ĩa**−**IĨIa** of complexes **Ia**−**IIIa**. The LanL2DZ basis set was used for all calculations, which applies Dunning/Huzinaga full double zeta (D95)[24] basis functions on first row and Los Alamos effective core potentials plus DZ functions on all other atoms.[25] This basis set proved to be superior to 3-21G or 3-21G** in comparative calculations for the systems under investigation. Convergence was reached when the relative change in the density matrix between subsequent iterations was less than 1×10^{-5} for single points and 1×10^{-8} for optimizations. Charges were analyzed using the natural bond orbital (NBO) formalism.[26] All computational procedures were used as they are implemented in the Gaussian94 E.1 package.[27] Wavefunctions were plotted with the visualization program Molden,[28] and the force constants in internal coordinates were extracted from the Gaussian output using the program Redong.[29]

The structures of the models (**Ĩa**−**IĨIa**) used for calculation (cf. Table 1 and Figure 1) are derived from existing complexes but simplified by setting all valence angles at the metal atoms to 90° and taking the Mo−N−N moiety as linear. Furthermore, the coordinating phosphorus atoms are saturated with hydrogen. The bond lengths and angles of the hydrogen atoms in the resulting "new" PH_3 ligands are based on the known data of the free molecule. The PH_3 groups are adjusted in a way that the highest possible molecular symmetry is reached. For the model systems **Ĩa** and **IĨIa**, all other bond lengths are taken from X-ray structures (cf. Table 1). The crystal structure of compound **II** is not known. Therefore, the coordinates of **IĨIa** are based on a geometry optimization (cf. Table 1). The structures of the model systems **Ĩa**−**IĨIa** are given in Figure 1. The NNH angle of **IĨIa** is chosen in accordance with X-ray crystallography and that of **IĨIa** is taken from a geometry optimization. The d orbitals in all model systems are oriented in a way that $d_{x^2-y^2}$ gives rise to π and d_{xy} to σ interaction with ligand (phosphorus) orbitals. As this is opposed to the usual bonding situation in octahedral complexes, we exchanged the labels of these orbitals in order to make the MO analysis easier to access.

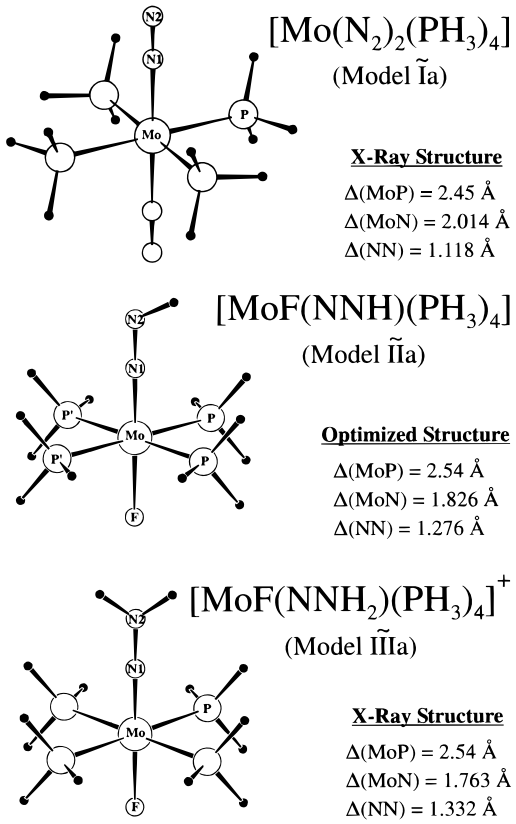

Figure 1. Structures of the model systems **Ĩa**, **IĨa**, and **IĨIa** used for calculation.

The MO schemes of the free ligands N_2, NNH^-, NNH_2, and, for comparison, *trans*-HNNH have been calculated as well. The structures of N_2 and HNNH[31] are those of the free molecules, whereas optimized structures are used for NNH^- and NNH_2.

Results and Analysis

A. DFT Calculations. Frontier Orbitals of the Free Ligands. The highest occupied and lowest unoccupied orbitals

(22) (a) Dilworth, J. R.; Richards, R. L. *Inorg. Synth.* **1980**, *20*, 119. (b) See refs 10d and e.
(23) Becke, A. D. *J. Chem. Phys.* **1993**, *98*, 5648.
(24) Dunning, T. H., Jr.; Hay, P. J. In *Modern Theoretical Chemistry*; Schaefer, H. F., III, Ed.; Plenum: New York, 1976.
(25) (a) Hay, P. J.; Wadt, W. R. *J. Chem. Phys.* **1985**, *82*, 270 and 299. (b) Wadt, W. R.; Hay, P. J. *J. Chem. Phys.* **1985**, *82*, 284.
(26) (a) Foster, J. P.; Weinhold, F. *J. Am. Chem. Soc.* **1980**, *102*, 7211. (b) Rives, A. B.; Weinhold, F. *Int. J. Quantum Chem. Symp.* **1980**, *14*, 201. (c) Reed, A. E.; Weinstock, R. B.; Weinhold, F. *J. Chem. Phys.* **1985**, *83*, 735. (d) Reed, A. E.; Curtiss, L. A.; Weinhold, F. *Chem. Rev.* **1988**, *88*, 899.
(27) Frisch, M. J.; Frisch, Æ.; Foresman, J. B. *Gaussian 94 User's Reference*; Gaussian Inc.: Carnegie Office Park, Building 6, Pittsburgh, PA 15106; 1994.
(28) Schaftenaar, G. *Molden*, version 3.2; CAOS/CAMM Center, University of Nijmegen: The Netherlands.
(29) Allouche, A.; Pourcin, J. *Spectrochim. Acta* **1993**, *49A*, 571.
(30) (a) Uchida, T.; Uchida, Y.; Hidai, M.; Kodama, T. *Acta Crystallogr.* **1975**, *B31*, 1197. (b) Hidai, M.; Kodama, T.; Sato, M.; Harakawa, M.; Uchida, Y. *Inorg. Chem.* **1976**, *15*, 2694.
(31) Carlotti, M.; Johns, J. W. C.; Trombetti, A. *Can. J. Phys.* **1974**, *52*, 340.

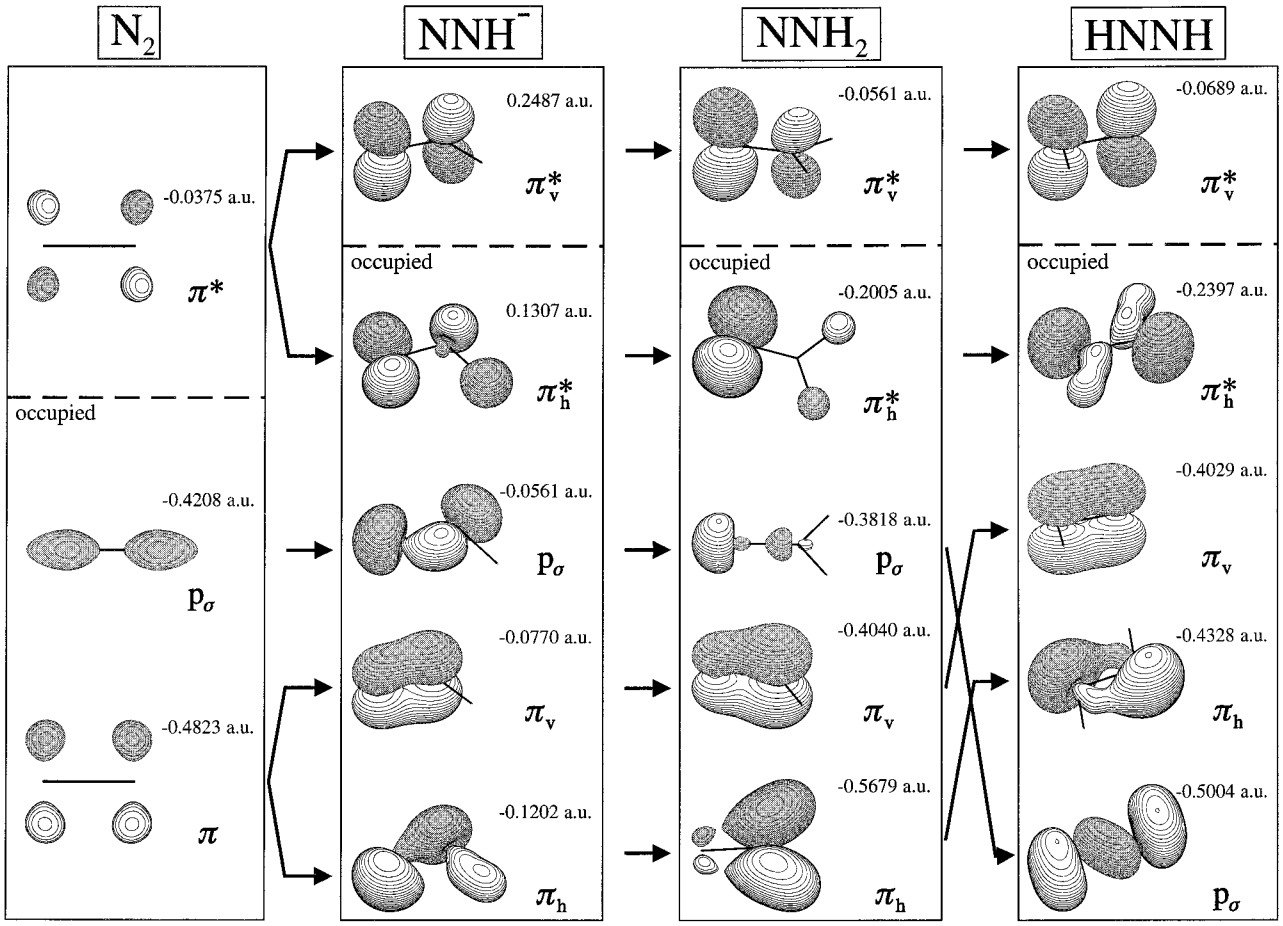

Figure 2. Contours of the molecular orbitals of the free ligands and their correlation.

of N_2, NNH^- (diazenide), NNH_2 (isodiazene), and *trans*-HNNH (diazene) are shown in Figure 2. Free dinitrogen has a set of two degenerate π^* orbitals which are the lowest unoccupied orbitals (LUMOs) of the molecule. The splitting between π and π^* is very large because of the short bond distance and the strong overlap of the involved p functions. The HOMO of N_2 is p_σ, a lone pair formed by the nearly nonbonding combination of two sp hybrids.

The bonding of a proton removes the degeneracy of the two π bonds of N_2 and leads upon further addition of two electrons to the nonexisting NNH^- (diazenide) species. Due to the negative charge, the whole MO scheme is shifted to higher energy. In the following, π_v (vertical) labels the orbitals which are perpendicular to the NNH plane and correspond to "real" π bonds whereas π_h (horizontal) orbitals lie within the NNH plane and derive from the p functions of the nitrogen atoms which are directed to hydrogen atoms. The LUMO of diazenide, π^*_v, is very similar to the π^* orbitals of N_2 whereas the in-plane π interaction is distinctly weakened by the bonding of a hydrogen atom. Correspondingly, the HOMO π^*_h has a much larger p coefficient on the coordinating than on the terminal nitrogen atom giving this orbital the properties of a p donor which is weakly coupled to the terminal NH group. At the NNH_2 stage, the residual coupling breaks apart leading to a covalent N−H bond (orbital π_h; cf. Figure 2) and a p donor orbital at the coordinating nitrogen labeled π^*_h. In contrast, the LUMO π^*_v again remains nearly unchanged. For comparison, the orbitals of diazene are shown in Figure 2 as well. Whereas isodiazene acts as a p donor with π^*_h, the corresponding orbital of *trans*-diazene mediates a σ donor interaction.[17] In addition, diazene has two equivalent coordination sites and therefore strongly prefers a bridging or side-on geometry[18] whereas isodiazene forms a linear π bond. Hence, diazene is an intermediate of the symmetric and isodiazene of the asymmetric reduction pathway.

The bonding interactions between the NNH_x ($x = 0-2$) ligands and metals are mostly mediated by their respective HOMOs and LUMOs; all other orbitals have much weaker bonding capabilities. In the following, the molybdenum−N_2, −NNH, and −NNH_2 complexes are considered in detail. The structures of the corresponding model systems **Ĩa**, **IĨa**, and **IĨIa** are given in Tables 2a, 3a, and 4a, and orbital decompositions are given in Tables 2b, 3b, and 4b, respectively. The corresponding MO schemes are combined in Figure 3; relevant orbital plots are shown in Figures 4 (**Ĩa**), 5 (**IĨa**), and 6 (**IĨIa**).

Dinitrogen Complex of Mo. The bis(dinitrogen) complex **Ia** has a linear N−N−Mo−N−N unit that is strongly conjugated. Importantly, both HOMO and LUMO of the corresponding model **Ĩa** belong to this π system (cf. Figure 3). The occupied t^*_{2g} orbitals d_{xz}–$\pi^*_x\langle 37\rangle$ and d_{yz}–$\pi^*_y\langle 35\rangle$ comprising the HOMO derive from the *bonding* combinations of d_{xz} and d_{yz} with the N_2 π^* orbitals (cf. Figure 4). The 25% N_2 contribution to these orbitals indicates relatively strong backbonding (cf. Table 2b). The third t^*_{2g} orbital, d_{xy}, is nonbonding with respect to dinitrogen and phosphorus but shows some hydrogen admixture. The LUMOs of **Ĩa**, π^*_x(nb)$\langle 39\rangle$ and π^*_y(nb)$\langle 38\rangle$, derive from the in-phase combinations of the dinitrogen π^* orbitals. Apart from a little admixture of molybdenum p functions, they are Mo−N *nonbonding* and effectively correspond to the π^* orbitals of free N_2. The *antibonding* combinations of d_{yz} and d_{xz} with π^*, π^*_x–$d_{xz}\langle 47\rangle$, and

Table 2

(a) Coordinates of the Asymmetric Unit of $[Mo(N_2)_2(PH_3)_4]$ (**Ĩa**)[a]

no.	atom	position (x, y, z)[b]		
1	Mo	0.000	0.000	0.000
2	N1	0.000	0.000	2.014
3	N2	0.000	0.000	3.132
4	P	0.000	2.450	0.000
5	H1	−1.270	3.080	0.000
6	H11	0.640	3.080	1.100
7	H21	0.640	3.080	−1.100

(b) Charge Contributions of $[Mo(N_2)_2(PH_3)_4]$ (**Ĩa**)[c]

orbital	label	energy (Hartree)	charge decomposition[d] % N1[e]	% N2[e]	% Mo	% P	% H
d_{z^2}	$a_g\langle 55\rangle$	0.1075	22	3	38	29	8
	$b_{2g}\langle 53\rangle$	0.0870	1	1	7	44	47
	$b_{3g}\langle 52\rangle$	0.0737	3	2	13	42	40
$d_{x^2-y^2}$	$b_{1g}\langle 48\rangle$	0.0491	0	0	29	68	3
π^*_x–d_{xz}	$b_{2g}\langle 47\rangle$	0.0489	37	27	12	10	15
π^*_y–d_{yz}	$b_{3g}\langle 46\rangle$	0.0438	26	18	3	24	29
PH_3	$a_g\langle 43\rangle$	0.0241	7	10	35	35	14
PH_3	$b_{1u}\langle 42\rangle$	0.0215	2	0	1	43	55
π^*_x (nb)	$b_{3u}\langle 39\rangle$	−0.0114	29	39	8	20	3
π^*_y (nb)	$b_{2u}\langle 38\rangle$	−0.0122	28	38	8	20	6
d_{xz}–π^*_x	$b_{2g}\langle 37\rangle$	−0.1544	3	24	65	0	9
d_{xy}	$a_g\langle 36\rangle$	−0.1561	0	0	67	3	30
d_{yz}–π^*_y	$b_{3g}\langle 35\rangle$	−0.1591	2	23	60	2	13
PH_3	$b_{2u}\langle 34\rangle$	−0.2813	0	3	9	79	9
PH_3	$b_{3u}\langle 33\rangle$	−0.2813	0	2	9	79	9
$d_{x^2-y^2}$	$b_{1g}\langle 32\rangle$	−0.3195	0	0	26	65	9
d_{z^2}	$a_g\langle 31\rangle$	−0.3550	2	1	12	68	10
p_σ (nb)	$b_{1u}\langle 30\rangle$	−0.3771	31	58	4	2	3
	$b_{1g}\langle 29\rangle$	−0.3984	0	0	0	40	60
p_σ–d_{z^2}	$a_g\langle 28\rangle$	−0.3987	20	72	2	0	3
	$b_{3g}\langle 27\rangle$	−0.4060	16	15	0	29	40
	$b_{2g}\langle 26\rangle$	−0.4075	21	18	0	24	37
	$b_{3u}\langle 25\rangle$	−0.4094	7	6	1	40	46
	$b_{2u}\langle 22\rangle$	−0.4236	13	10	0	31	46
π_y (nb)	$b_{2u}\langle 21\rangle$	−0.4300	50	36	1	7	6
π_x (nb)	$b_{3u}\langle 20\rangle$	−0.4303	53	38	1	4	3
π_y–d_{yz}	$b_{3g}\langle 18\rangle$	−0.4424	50	31	3	10	7
π_x–d_{xz}	$b_{2g}\langle 17\rangle$	−0.4448	46	29	3	11	11
σ^* (nb)	$b_{1u}\langle 16\rangle$	−0.5240	64	28	8	1	0
σ^*–d_{z^2}	$a_g\langle 15\rangle$	−0.5724	69	24	7	1	0

[a] The missing coordinates are generated by the use of symmetry operations like inversion and reflection (**Ĩa** has D_{2h} symmetry). [b] Coordinates of the atoms in Å. [c] Only selected orbitals are listed. [d] If several symmetry-equivalent atoms exist, the charge decomposition gives the sum of all contributions. [e] N1 is the coordinating and N2 the terminal nitrogen atom.

π^*_y–$d_{yz}\langle 46\rangle$ (cf. Figure 4), are located at distinctly higher energy than the LUMOs reflecting again the strong degree of backbonding between dinitrogen and molybdenum. In contrast, the σ interaction between molybdenum d_{z^2} and the p_σ HOMO of dinitrogen is weak. This is indicated by the charge decomposition of the corresponding orbital p_σ–$d_{z^2}\langle 28\rangle$ (cf. Figure 4) containing only 2% metal contribution (cf. Table 2b). Although the σ^* orbital of N_2 is at much lower energy, its overlap with Mo is somewhat larger (decomposition of σ^*–$d_{z^2}\langle 15\rangle$: 7% Mo, 92% N_2).

This bonding description is supported by the NPA (Natural Population Analysis) charges (Table 5) and d orbital populations (Table 6). The relatively strong backbonding interactions are reflected by d_{xz} and d_{yz} populations of 1.5 as compared to the population of 1.8 of d_{xy} which is nonbonding. Including the contributions of π backbonding and σ donation to the Mo center, the N_2 ligand acquires a total charge of −0.13.

NNH Complex of Mo. In the singly protonated species **IIa**, one dinitrogen ligand is replaced by fluoride leading to a F−Mo−N−N(H) moiety. Whereas the N−N distance increases (cf. Table 1), the Mo−N bond is shortened with respect to the parent complex **Ia**. Because of the enlargement of the N−N distance, the out-of-plane π^*_v orbital of NNH is at lower energy than the corresponding π^* orbital of dinitrogen. As a consequence, the backbonding interaction with the metal d_{xz} orbital is strengthened which is also reflected by the decomposition of the bonding combination d_{xz}–$\pi^*_v\langle 35\rangle$ (33% N_2 and 47% Mo vs 27% N_2 and 65% Mo in d_{xz}–π^*_x of the N_2 complex; cf. Table 3b and Figure 5). This orbital is the HOMO of the complex. Strong mixing also occurs between d_{yz} and the in-plane π^*_h orbital of NNH which is lower in energy than π^*_v due to the interaction with hydrogen. The bonding combination (π^*_h–d_{yz}) has 54% NNH and 28% Mo character and therefore a preponderance of π^*_h. This represents an "inverted" bonding situation with respect to the parent N_2 complex which is accounted for by the π^*_h–d_{yz} labeling. Correspondingly, the antibonding orbital d_{yz}–π^*_h which is the LUMO of model complex **IĨIa** has a major d_{yz} participation (cf. Figure 3). Both in-plane and out-of-plane backbonding orbitals also contain antibonding contributions of fluorine p functions.

The occupation of π^*_h–d_{yz} is equivalent with the formation of a rather covalent in-plane Mo−N π bond which is also reflected by the d_{yz} population being lowered to a value of 0.95. As indicated by the d_{xz} occupation of 1.37, the out-of-plane π interaction is comparatively weaker, but nevertheless strengthened with respect to the N_2 complex (vide supra). Including the electron density donated to the metal center by π^*_h and received from the metal via π^*_v, the NNH ligand is predicted to acquire a total charge of −0.39. From a comparison of the calculated and experimentally determined N−N force constants of this species (9.48 vs 8.27 mdyn/Å), however, the negative charge imposed on NNH must be higher (see below).

NNH_2 Complex of Mo. For comparison with free isodiazene, the MO scheme of **IĨIa** given in Figure 3 has been shifted to higher energy to compensate for the offset due to the positive charge of the complex. Addition of H^+ to complex **IIa** leading to the doubly protonated species **IIIa** causes a further shortening of the Mo−N bond which is accompanied by an enlargement of the N−N distance. This causes a further decrease of the π^*_v orbital in energy thus increasing the contribution of π^*_v to the bonding combination d_{xz}–π^*_v to 50%. The remaining 50% are made up by metal (30%), F (11%), and PH_3 contributions. In spite of the antibonding fluorine p admixture, this orbital is still at lower energy than d_{xy} which is nonbonding (Figure 3). The NPA analysis now gives a value of 1.11 for d_{xz} indicative of a maximum degree of covalency for the out-of-plane π bond at this stage. In fact, this interaction is comparable to the in-plane interaction in the NNH complex.

As mentioned above, the π^*_h orbital now has the properties of a p lone pair which is responsible for the p donor capability of NNH_2 (cf. Figure 2). The bonding combination π^*_h–d_{yz} is split into $b_2\langle 33\rangle$ and $b_2\langle 31\rangle$ (not shown) by interaction with phosphine (cf. Table 4b). As reflected by the small molybdenum-d participations, π^*_h is now clearly lower in energy than d_{yz}. In fact, this inverted bonding situation is now even more pronounced than in **IIa** (see above) which is also indicated by the d_{yz} population being lowered to 0.73. The corresponding antibonding combination d_{yz}–$\pi^*_h\langle 36\rangle$, which is metal dominated, is the LUMO of model **IIIa** (cf. Figures 3 and 6).

Via its p donor capacity, NNH_2 loses charge to the metal

Table 3

(a) Coordinates of the Asymmetric Unit of [MoF(NNH)$(PH_3)_4$] (**ĨIa**)[a]

no.	atom	position (x, y, z)[b]			no.	atom	position (x, y, z)[b]		
1	Mo	0.000	0.000	0.000	8	H11	0.640	3.170	1.100
2	F	0.000	0.000	−2.070	9	H21	0.640	3.170	−1.100
3	N1	0.000	0.000	1.826	10	P′	0.000	−2.540	0.000
4	N2	0.000	0.000	3.102	11	H2	1.270	−3.170	0.000
5	H1(N)	0.673	0.673	3.545	12	H31	−0.640	−3.170	−1.100
6	P	0.000	2.540	0.000	13	H41	−0.640	−3.170	1.100
7	H1	−1.270	3.170	0.000					

(b) Charge Contributions of [MoF(NNH)$(PH_3)_4$] (**ĨIa**)[c]

orbital	label	energy (Hartree)	charge decomposition[d]								
			% N1[e]	% N2[e]	% H	% Mo	% F	% P	% P′	% H	% H′
d_{z^2}	a′⟨51⟩	0.1051	17	2	0	34	3	14	14	8	9
PH_3	a′⟨45⟩	0.0506	3	0	0	55	0	12	11	9	9
PH_3	a′⟨44⟩	0.0458	0	2	0	26	0	14	21	13	22
$d_{x^2-y^2}$	a″⟨41⟩	0.0212	1	1	0	33	0	28	34	2	2
π^*_v–d_{xz}	a″⟨40⟩	0.0200	19	11	0	23	1	20	9	10	8
	a′⟨39⟩	0.0173	0	0	0	4	1	20	19	27	26
d_{yz}–π^*_h	a′⟨36⟩	−0.0078	25	9	11	36	3	3	3	6	4
d_{xz}–π^*_v	a″⟨35⟩	−0.1476	3	30	0	47	9	2	2	3	3
d_{xy}	a′⟨34⟩	−0.1683	0	0	0	74	0	1	1	12	11
π^*_h–d_{yz}	a′⟨33⟩	−0.1794	16	31	7	28	8	4	4	1	1
$F(p_x) + \pi_v$	a″⟨32⟩	−0.2676	3	5	0	6	42	20	21	2	2
$F(p_y) + \pi_h$	a′⟨31⟩	−0.2705	2	8	0	7	44	17	18	2	2
$F(p_z)$	a′⟨30⟩	−0.2925	8	2	1	9	79	0	0	0	1
$F(p_y)$	a′⟨29⟩	−0.2998	0	0	0	10	41	20	21	3	3
$F(p_x)$	a″⟨28⟩	−0.2999	0	0	0	10	44	17	21	3	4
$d_{x^2-y^2}$	a″⟨27⟩	−0.3205	0	0	0	25	0	36	30	5	4
π_h–d_{yz}	a′⟨26⟩	−0.3467	44	36	0	7	4	1	2	2	2
π_v–d_{xz}	a″⟨25⟩	−0.3527	53	29	0	8	0	2	2	3	3
d_{z^2}	a′⟨24⟩	−0.3565	0	0	0	18	0	37	33	5	5
p_σ–d_{z^2}	a′⟨15⟩	−0.4597	46	26	9	12	2	1	0	1	0

[a] The missing coordinates are generated by reflection (**ĨIa** has C_s symmetry). [b] Coordinates of the atoms in Å. [c] Only selected orbitals are listed. [d] If several symmetry-equivalent atoms exist, the charge decomposition gives the sum of all contributions. [e] N1 is the coordinating and N2 the terminal nitrogen atom.

but, on the other hand, receives electron density from the metal by strong back-donation via π^*_v. These two contributions effectively cancel leaving the ligand with a slightly negative charge (−0.03 from NPA, see below and Table 5). In contrast, the "hydrazido(2−)" formulation assigns the whole charge of d_{xz}–π^*_v and π^*_h–d_{yz} to the NNH_2 ligand giving a too ionic description of the Mo−N bond. Therefore, NNH_2 is coordinated as covalently bound isodiazene.

By means of p_σ, isodiazene is a stronger σ donor than N_2 or NNH. This is evident from the strong energetic depression of p_σ–d_{z^2}⟨16⟩ which is due to interaction with the metal−d_{z^2} orbital. This compensates for the loss of hydrogen bonding character as compared to the analogous orbital of **ĨIa** which is also found at deep binding energy, however primarily due to an N−H bonding interaction.

B. Comparison to Spectroscopy. Optical Absorption: Charge-Transfer Transitions. The UV−vis spectra of the dinitrogen complexes [W$(N_2)_2$(dppe)$_2$] (**Ib**, Figure 7) and [Mo$(N_2)_2$(dppe)$_2$] (**Ia**, spectrum not shown) are quite similar and exhibit a strong absorption at 298 and 307 nm, respectively, and a broader, but less intense, band at 380 nm. In contrast, the spectrum of [W$(N_2)_2$(depe)$_2$] (Figure 8) only contains the corresponding strong absorption at 310 nm but no feature comparable with the 380 nm band of the dppe systems which therefore must be assigned to a transition directly involving the dppe ligands but not the M−N_2 moiety. George et al. attribute this feature to an electronic transition from metal d to phosphine d orbitals. In the depe system, this band is blue-shifted[32] and masked by the strong absorption at 310 nm. As in the case of the analogous Mo compound, the spectrum of the W−N_2 depe complex exhibits some weak bands (cf. ref 33) at 498, 455, ∼390, and ∼360 nm which are assigned to ligand field transitions (Figure 8, detailed analysis see below). Unfortunately, these features are masked by the broad 380 nm band in case of the dppe complexes. In the protonated species [WF(NNH)(dppe)$_2$] (**IIb**) and [WF(NNH_2)(dppe)$_2$](BF_4) (**IIIb**), the broad absorption band related to the dppe ligands is shifted to 325 nm and no other feature can be detected down to 250 nm. Based on the MO schemes of models **Ĩa**−**ĨIIa** (Figure 3) and in agreement with George et al.,[32] the strong absorption band at about 300 nm of the dinitrogen complexes is assigned to the symmetry-allowed metal to ligand charge transfer transitions d_{yz}–$\pi^*_y \rightarrow \pi^*_y$(nb) and d_{xz}–$\pi^*_x \rightarrow \pi^*_x$(nb) which are of comparable energy. The nonbonding orbitals π^*_y(nb) and π^*_x(nb) are a special feature of the linear N−N−M−N−N moiety appearing at distinctly lower energy than the antibonding metal-π* combinations. Therefore, the corresponding orbital energy differences are smaller (∼31 800 $cm^{-1} \equiv$ 315 nm for the nonbonding versus ∼44 500 $cm^{-1} \equiv$ 225 nm for the antibonding combinations) and in fact show good agreement with the measured band position. Furthermore, the large intensity of this absorption supports the given assignment to a symmetry-allowed

(32) (a) George, T. A.; Busby, D. C.; Iske, S. D. A., Jr. *Inorg. Organomet. Photochem.* **1978**, 147. (b) Bossard, G. E.; Busby, D. C.; Chang, M.; George, T. A.; Iske, S. D. A., Jr. *J. Am. Chem. Soc.* **1980**, *102*, 1001.
(33) Caruana, A.; Kisch, H. *Angew. Chem.* **1979**, *91*, 335.

Table 4

(a) Coordinates of the Asymmetric Unit of $[MoF(NNH_2)(PH_3)_4]^+$ (**IĨIa**)[a]

no.	atom	position (*x*, *y*, *z*)[b]			no.	atom	position (*x*, *y*, *z*)[b]		
1	Mo	0.000	0.000	0.000	6	H2(N)	−0.630	−0.630	3.720
2	F	0.000	0.000	−1.990	7	P	0.000	2.540	0.000
3	N1	0.000	0.000	1.763	8	H1	−1.270	3.170	0.000
4	N2	0.000	0.000	3.095	9	H11	0.640	3.170	1.100
5	H1(N)	0.630	0.630	3.720	10	H21	0.640	3.170	−1.100

(b) Charge Contributions of $[MoF(NNH_2)(PH_3)_4]^+$ (**IĨIa**)[c]

			charge decomposition[d]						
orbital	label	energy (Hartree)	% N1[e]	% N2[e]	% H	% Mo	% F	% P	% H
d_{z^2}	$a_1\langle 50\rangle$	−0.0548	30	4	1	27	3	18	14
	$a_1\langle 39\rangle$	−0.1309	2	19	6	34	1	26	13
$d_{x^2-y^2}$	$a_2\langle 38\rangle$	−0.1368	0	0	0	36	0	63	2
π_v^*–d_{xz}	$b_1\langle 37\rangle$	−0.1561	36	12	0	33	4	7	9
d_{yz}–π_h^*	$b_2\langle 36\rangle$	−0.1848	20	2	13	53	5	2	4
d_{xy}	$a_1\langle 35\rangle$	−0.3356	0	0	0	84	0	0	15
d_{xz}–π_v^*	$b_1\langle 34\rangle$	−0.3467	14	35	0	30	11	8	2
π_h^*–d_{yz}	$b_2\langle 33\rangle$	−0.3977	26	1	3	7	19	39	4
$F(p_x) + \pi_v$	$b_1\langle 32\rangle$	−0.4233	0	11	0	9	11	62	7
π_h^*–d_{yz}	$b_2\langle 31\rangle$	−0.4519	28	2	5	19	3	34	7
$F(p_z)$	$a_1\langle 30\rangle$	−0.4682	9	3	0	9	77	1	1
$F(p_x)$	$b_1\langle 29\rangle$	−0.4683	0	1	0	11	76	7	4
$F(p_y)$	$b_2\langle 28\rangle$	−0.4705	6	1	1	16	69	3	4
$d_{x^2-y^2}$	$a_2\langle 27\rangle$	−0.4713	0	0	0	35	0	56	9
d_{z^2}	$a_1\langle 26\rangle$	−0.5051	0	0	0	25	1	62	11
π_v–d_{xz}	$b_1\langle 25\rangle$	−0.5245	35	36	0	5	0	9	14
p_σ–d_{z^2}	$a_1\langle 16\rangle$	−0.6437	51	24	3	19	4	0	0
π_h (nb)	$b_2\langle 15\rangle$	−0.6559	10	66	22	1	0	0	0

[a] The missing coordinates are generated by reflections (**IĨIa** has C_{2v} symmetry). [b] Coordinates of the atoms in Å. [c] Only selected orbitals are listed. [d] If several symmetry-equivalent atoms exist, the charge decomposition gives the sum of all contributions. [e] N1 is the coordinating and N2 the terminal nitrogen atom.

charge transfer transition. In case of the protonated species, no such nonbonding orbitals exist and accordingly, no corresponding spectral features can be detected down to 250 nm (cf. Figure 7). This is in agreement with the calculated energy differences between the bonding and antibonding combinations of d_{xz} with π_v^* (the in-plane orbitals in general have even larger splittings) predicting these absorptions to appear distinctly below 300 nm.

Optical Absorption: Ligand Field Transitions. The observed ligand field bands of $[W(N_2)_2(depe)_2]$ (Figure 8) can be related to electronic transitions within a d^6 low-spin system with octahedral environment. For an analysis of the ligand field spectrum, we applied angular overlap model (AOM) calculations[34] to a $[W(N)_2(P)_4]$ model system of D_{4h} symmetry with six formal ligands (two of "N" type and four of "P" type). The real dinitrogen complex has a lower symmetry because of the bidentate depe ligands and distortions from ideal geometry. Thus, the absorption bands at 20 080 $cm^{-1} \equiv 498$ nm and 21 980 $cm^{-1} \equiv 455$ nm can be assigned to transitions from the $^1A_{1g}$ ground state to the two terms ^1E_g and $^1A_{2g}$ of $^1T_{1g}$ split in D_{4h}. Accordingly, the bands at ~25 500 $cm^{-1} \equiv 390$ nm and ~27 600 $cm^{-1} \equiv 360$ nm belong to the $^1B_{2g}$ and ^1E_g components of $^1T_{2g}$. In terms of the AOM parameters listed in Table 7, the energetic sequence of the different split terms is predominantly related to the difference in e_σ between the axial and equatorial ligands and otherwise practically independent of the choice of parameters.

Both absorption bands resulting from $^1T_{1g}$ at 20 080 (^1E_g) and 21 980 cm^{-1} ($^1A_{2g}$) exhibit the same vibrational structure of about 410 cm^{-1} when measured in a KBr disc at 10 K (cf. Figure 8). The involved vibration has to be totally symmetric and, due to its frequency, of metal−ligand stretching type. From our vibrational studies this mode has to be assigned to the symmetric W−N stretch (419/414 cm^{-1}, cf. Part I of this series). Nevertheless, this is difficult to reconcile with the above assignments as in a strong-field scheme $^1A_{1g} \rightarrow {}^1E_g(^1T_{1g})$ corresponds to $d_{xz}/d_{yz} \rightarrow d_{z^2}$ and $^1A_{1g} \rightarrow {}^1A_{2g}(^1T_{1g})$ to $d_{xy} \rightarrow d_{x^2-y^2}$. Both orbitals involved in the latter transition, however, are nonbonding with respect to N_2 making a displacement in the W−N vibration difficult to understand. Alternatively, both visible $^1T_{1g}$ bands are attributed to components of $^1A_{1g} \rightarrow {}^1E_g$ split by the rhombic distortion of the complex due to the bidentate phosphine ligands and/or a Jahn−Teller effect. In that case, however, the question arises where $^1A_{1g} \rightarrow {}^1A_{2g}$ is located; possibly, this transition is shifted to much higher energy (i.e. into the region of the $^1T_{2g}$ transitions) due to the large σ donating effect of the equatorial phosphine groups. At present, this question cannot be decided convincingly without more detailed, preferentially low-temperature single-crystal measurements.

Vibrational Spectroscopy. Calculated and observed N−N and M−N stretching and M−N−N bending frequencies are listed in Table 8. In case of the Mo− and W−N_2 systems, excellent agreement with experiment is achieved, especially for ν(NN) (average deviation from experiment: 11 cm^{-1}). In contrast, the calculated frequencies obtained by applying DVXα on comparable model systems are about 500 cm^{-1} too low.[36] For both protonated species, the deviations are larger but the obtained values are still close to experiment.

The same trends are evident from the corresponding force constants given in Table 9. In case of the W−N_2 and the NNH_2 system, the calculated values are in very good agreement with the QCA−NCA results (see Part I of this series) providing further evidence that for these compounds a good theoretical description has been achieved with the chosen method. In contrast, the results for the NNH system are of somewhat lower quality as the calculated N−N force constant is distinctly larger than experimentally determined. Therefore, the N−N bond order is overestimated and the NNH ligand more negatively charged, i.e. closer to diazenido(−) than calculated.

Discussion

The calculations presented in this paper allow an analysis of the electronic-structural contributions to the first two protonations of metal-bound N_2 along the asymmetric pathway. This is of relevance with respect to an understanding of biological nitrogen fixation as well as the realization of a corresponding synthetic process at room temperature and ambient pressure. As outlined in the Introduction, there are two probable bonding modes of N_2 to the FeMoCo of nitrogenase which correspond to fundamentally different reduction modes. The end-on terminal coordination to an Fe_4-face of the FeMoCo entails a reduction along the asymmetric pathway involving bound −NNH, $-NNH_2$, and $-NNH_3$ species before splitting of the N−N bond and generation of NH_3. In contrast, reduction of N_2 being edge-on coordinated to this face most probably proceeds via sym-

(34) (a) Schmidtke, H. H. *Quantenchemie*; VCH Verlag: Weinheim, 1987 and references herein. (b) Adamsky, H. Ph.D. thesis, Universität Düsseldorf, Germany, 1995. (c) Adamsky, H.; Computer program *AOMX*, version dated from 01.02.1995; Institut für Theoretische Chemie, Universität Düsseldorf: Germany, 1995.

(35) Griffith, J. S. *The Theory of Transition-Metal Ions*; Cambridge University Press: London, 1971.

(36) Deeth, R. J.; Field, C. N. *J. Chem. Soc., Dalton Trans.* **1994**, 1943.

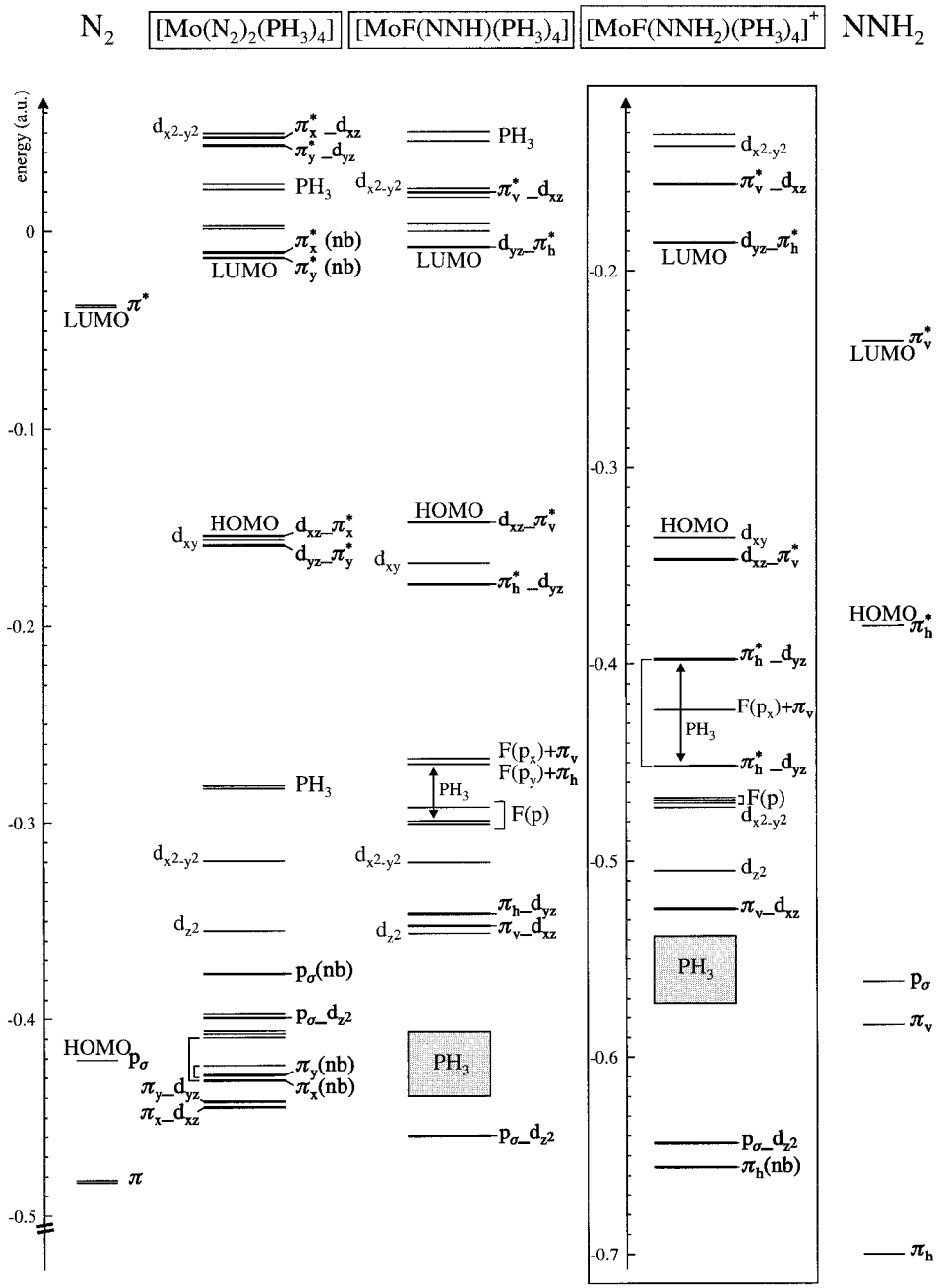

Figure 3. MO correlation diagram between free dinitrogen (left column), free isodiazene (right column), and models **Ĩa**, **ĨIa**, and **IĨIa**. MO designations correspond to those of Tables 2b, 3b, and 4b, respectively, and Figure 2.

metrically bound HNNH (diazene) and H_2NNH_2 (hydrazine) intermediates, i.e. along a symmetric pathway. Although the geometric and electronic structure of the FeMoCo is much more complex than that of simple mono- or bimetallic systems, it will be shown that salient features of both reduction modes can in fact be derived from these small-molecule systems. In the following, the implications of the obtained bonding descriptions with respect to the asymmetric reduction pathway will be discussed first. Then the reduction and protonation of symmetrically bound N_2 are considered briefly and both reduction modes are qualitatively compared to each other.

Bonding Descriptions of Mo/W−Nitrogenic Systems: Asymmetric Pathway. The first essential requirement for nitrogen fixation which applies to either pathway is a sufficient *activation* of the parent N_2 complex toward protonation. This term refers to the transfer of negative charge to the bound N_2 ligand via π back-donation from the metal d into the ligand π^* orbitals. On the other hand, charge is lost to the metal center via σ donation from N_2. Our DFT calculations on the Mo and W centers show that π backbonding from the t_{2g}^* orbitals is more important than σ donation leading to a net transfer of negative charge to the ligand. This was also concluded from EHMO[21] and SCF calculations.[37] The different computational methods, however, strongly affect the actual values of the calculated charges on the coordinating (N1) and terminal (N2) nitrogen atoms; in addition, the charge distribution depends on the applied analysis. Using DFT with the Natural Population Analysis (NPA) we obtained small and approximately identical negative charges on both nitrogen atoms, i.e. −0.07 on N1 and −0.06 on N2. For comparison, we also performed a Mulliken population analysis of the Mo−N_2 system giving a more negatively charged and

(37) Murrell, J. N.; Al-Derzi, A.; Leigh, G. J.; Guest, M. F. *J. Chem. Soc., Dalton Trans.* **1980**, 1425.

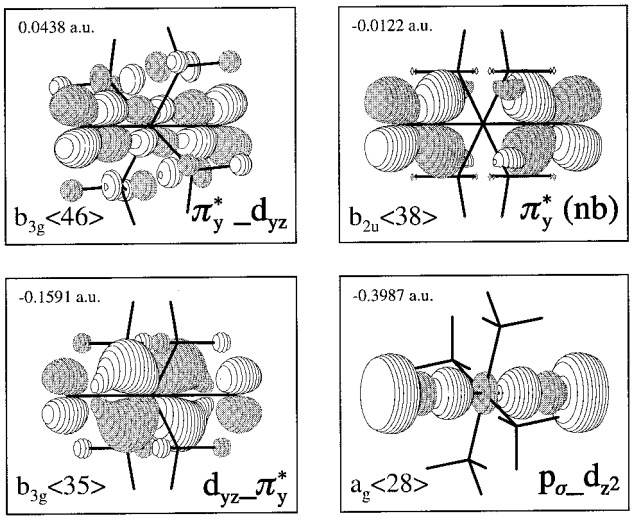

Figure 4. Contour plots of important molecular orbitals of **Ĩa**.

Table 5. NPA Charges of Mo Complexes

	atom						
complex	M	N1[a]	N2[a]	H[b]	P	P′	X
$[Mo(N_2)_2(PH_3)_4]$ (**Ĩa**)	−1.01	−0.07	−0.06	−	+0.31	−	−
$[MoF(NNH)(PH_3)_4]$ (**IĨa**)	−0.24	−0.17	−0.56	+0.34	+0.27	+0.28	−0.64
$[MoF(NNH_2)(PH_3)_4]^+$ (**IĨIa**)	+0.04	−0.21	−0.68	+0.43	+0.24	−	−0.55

[a] N1 is the coordinating and N2 the terminal nitrogen atom. [b] Charge for each H atom.

Table 6. NPA d Orbital Populations of Mo Complexes

	t_{2g}			e_g	
complex	d_{xz}	d_{yz}	d_{xy}	$d_{x^2-y^2}$	d_{z^2}
$[Mo(N_2)_2(PH_3)_4]$ (**Ĩa**)	1.51	1.51	1.76	1.05	0.82
$[MoF(NNH)(PH_3)_4]$ (**IĨa**)	1.37	0.95	*a*	0.95	*a*
$[MoF(NNH_2)(PH_3)_4]^+$ (**IĨIa**)	1.11	0.73	1.90	1.03	0.82

[a] "d_{xy}" and "d_{z^2}" are mixed from two different spheric harmonics and therefore it is not possible to give orbital populations (both orbitals contain 2.61 electrons in total).

more polarized N_2 unit with −0.06 on N1 and −0.11 on N2 which is in qualitative agreement with charges derived from the DVXα method.[36] In contrast, the EHMO calculations yield charges of +0.05 (N1) and −0.67 (N2), and a Mulliken analysis based on the mentioned SCF calculation even predicts an *inversely* polarized N_2 unit with −0.11 on N1 and −0.03 on N2. We found that a charge distribution with a strongly negative N2 atom is the result of very strong π backbonding whereas an inversely polarized N_2 is obtained if this interaction is weak as, e.g., in Fe(II)−N_2 systems.[38] It is therefore likely that the π interaction is overestimated by the EHMO and underestimated by the SCF method. This also follows from the fact that the orbital schemes resulting from EHMO exhibit much too small HOMO−LUMO gaps whereas the results from the SCF calculations for a model analogous to **Ĩa** give too large an energetic separation between the bonding and nonbonding combinations of π^*. In contrast, our energy level schemes correlate well with the observed optical absorption spectra of the Mo− and W−bis(dinitrogen) systems. In addition, the very good agreement between calculated and observed vibrational frequencies and force constants (cf. Part I of this series) makes us confident that our bonding description is reliable.

(38) Tuczek, F.; Wiesler, B. E.; Lehnert, N. Unpublished results.

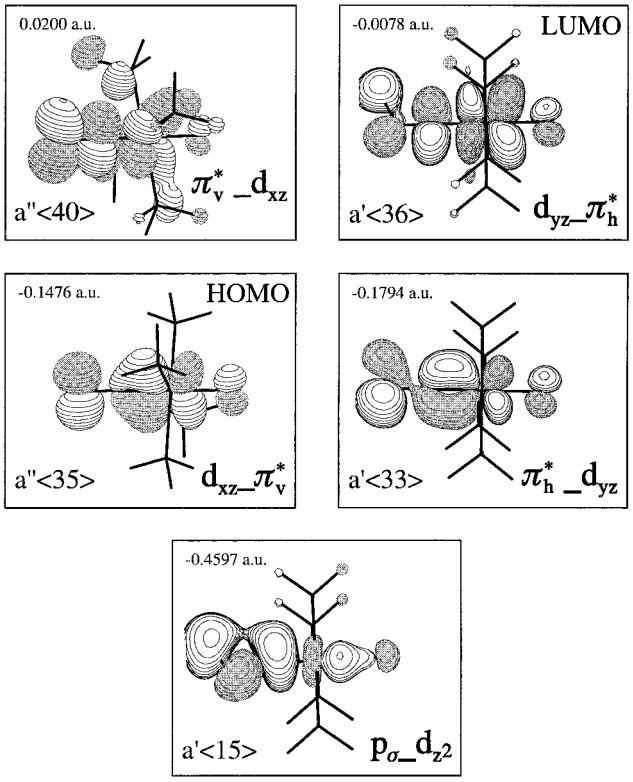

Figure 5. Contour plots of important molecular orbitals of **ĨIa**. For all in-plane orbitals, the same molecular orientation applies. The out-of-plane orbitals are shown from different perspectives.

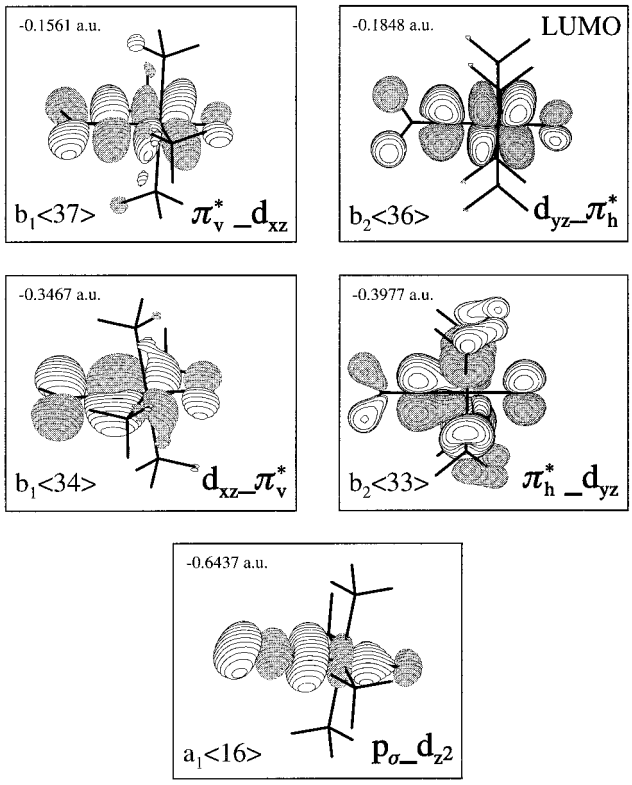

Figure 6. Contour plots of important molecular orbitals of **IĨIa**. For all in-plane orbitals, the same molecular orientation applies. The out-of-plane orbitals are shown from different perspectives.

The conversion of dinitrogen into diazene is a highly endothermic process (isodiazene and diazenide do not exist in free form). The second important role of the transition metal

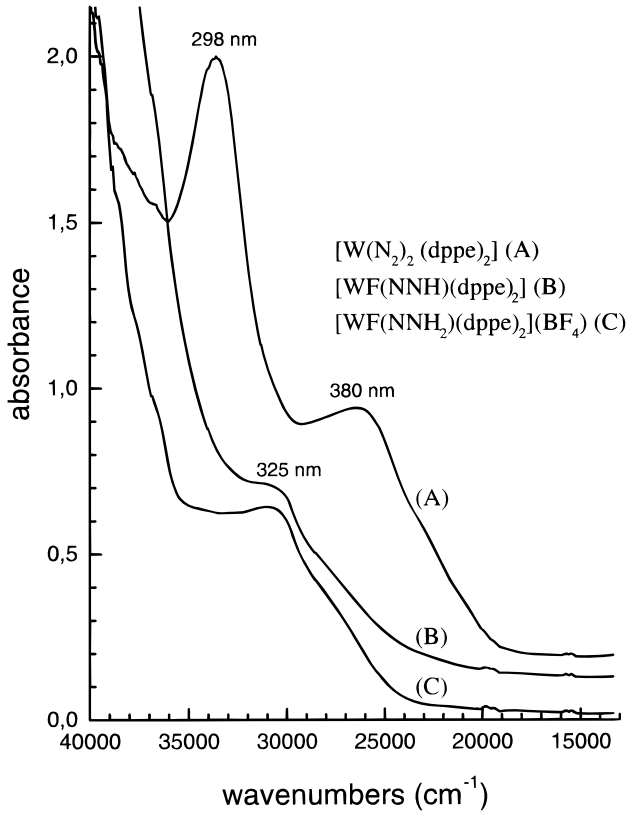

Figure 7. UV−vis spectra of the tungsten complexes **Ib**, **IIb**, and **IIIb** (as indicated) in THF at room temperature.

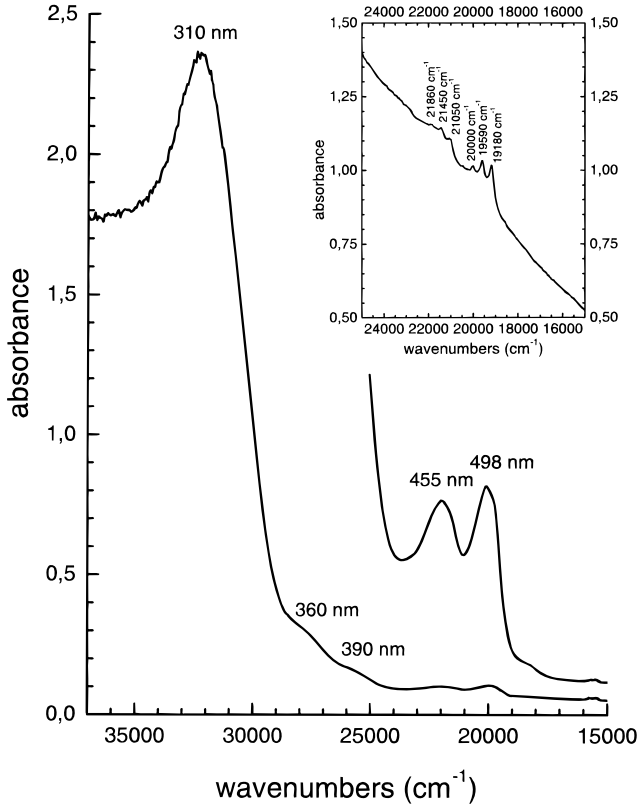

Figure 8. UV−vis spectrum of $[W(N_2)_2(depe)_2]$ in *n*-hexane at room temperature. The insert shows the ligand field transitions measured in a KBr disc at 10 K exhibiting a vibrational fine structure as indicated.

center is therefore to *stabilize* these species, i.e. provide a thermodynamic driving force for their generation (*basicity*). This is effected by an increase of *covalency* between the metal and the N_2H_x ($x = 0-2$) moitey following each protonation. As a consequence, the M−N bond is strengthened while N−N bond strength is decreased. From a mechanistic point of view, the weakening of the N−N bond initiates N_2 cleavage from the very first protonation step whereas the gradual increase of M−N bond strength acts to prevent loss of the partly reduced intermediates during the nitrogen fixation process. In addition, these reactions are accompanied by a *flow of electron density* from the metal d into the initially empty N_2 π^* orbitals compensating more or less for the charge withdrawal due to the addition of protons.

Table 7. Comparison of the Calculated and Observed Ligand Field Energies of $[W(N_2)_2(depe)_2]$ (in cm^{-1})

method	^1E_g	$^1A_{2g}$	$^1B_{2g}$	^1E_g
experimental[a]	20080	21980	25500	27600
AOM[b]	20150	22110	24700	26600

[a] Measured in *n*-hexane at room temperature. [b] Applying the following parameters: for the formal ligand "P", $e_\sigma(P) = 8000/e_\pi(P) = 600$; for "N", $e_\sigma(N) = 6900/e_\pi(N) = 500$; and $B = 400/C = 1600/\zeta = 2100$[35] (all parameters in cm^{-1}).

The calculations performed in this paper show how these requirements are met in the case of Mo/W−N_2 systems. After protonation of one of the N_2 ligands of the parent bis(dinitrogen) complex and loss of the second N_2, the interaction of the metal and ligand in-plane orbitals leads to the formation of one strong and covalent π bond. Out-of-plane back-donation is enhanced as well, but to a smaller degree. On the basis of NPA analysis the resulting NNH species has a charge of −0.4; the calculated N−N force constant is 9.48. From the experimentally determined force constant (8.27), however, the negative charge on this species must be higher, i.e. more toward −1 corresponding to the usual "diazenido(−)" formulation of this ligand (see below). Importantly, the terminal nitrogen atom is predicted to carry a strongly negative charge and thus can be further protonated without difficulty.

The MO scheme of the corresponding Mo-NNH_2 complex indicates that the interaction of d_{xz} with π_v^* is further increased such that a strong π bond perpendicular to the NNH_2 plane is formed. In contrast, the in-plane metal−ligand interaction is reduced since the π_h^* orbital now having the properties of a p donor is shifted below the metal d functions (inverted bonding scheme). Nevertheless, the net effect of both changes is still a slight increase in metal−ligand bond strength which is also reflected by an increase of the metal-N and a concomitant decrease of the N−N force constant. With a measured force constant of 7.2 in the coordinated NNH_2 group, the N−N interaction is reduced to a double bond at this stage, i.e. one π bond of dinitrogen has been completely removed and two electrons have been transferred to the N_2 moitey (cf. Table 9). The NNH_2 ligand therefore should be correctly designated as coordinated "isodiazene" and not as "hydrazido(2−)" having a single bond. In agreement with this description, the NNH_2 ligand carries virtually no net charge.

As apparent from these bonding descriptions, the transfer of electron density leading to the NNH_2 stage is distinctly smaller than during the first protonation step. Whereas the transformation of N_2 to NNH entails a major increase of covalency and is accompanied by a transfer of more than 1.4 electrons, the second protonation more or less corresponds to a normal acid−base reaction with a minor shift of electron density (<-0.6) from the metal to the ligand. Although the whole NNH_2 unit is almost neutral, its terminal nitrogen atom carries a negative partial charge. If the donor capacity of the metal site is sufficient (as in the case of the Mo/W-depe systems), a third protonation

Table 8. Observed and Calculated Frequencies (in cm^{-1}) of Mo/W Complexes

	ν(NN)			ν(MN)		δ(MNN)	
complex	exp.[a]	B3LYP[b]	DVXα[c]	exp.[a]	B3LYP[b]	exp.[a]	B3LYP[b]
$[W(N_2)_2(dppe)_2]$ (**Ib**)	2007 (s) 1948 (as)	1992 (s) 1953 (as)	1567 (s) –	419/414 (s) 435 (as)	452 (s) 437 (as)	 555 (as)	411/410 (s) 567/560 (as)
$[Mo(N_2)_2(dppe)_2]$ (**Ia**)	2033 (s) 1980 (as)	2015 (s) 1976 (as)	1441 (s) –	393/404 (s)	413 (s) 429 (as)	 550 (as)	385/384 (s) 570/557 (as)
$[MF(NNH)(dppe)_2]$ (**II**)[d]	1457	1563	–	(~530?)	614	514 (ip)	533 (ip)
$[MF(NNH_2)(dppe)_2]^+$ (**III**)[d]	1387	1451	–	581	627	510 (oop) 439 (ip)	560 (oop) 457 (ip)

[a] See Part I of this series; abbreviations: s and as are the corresponding symmetric and antisymmetric combinations; ip and oop are in-plane and out-of-plane bends relative to the M–N–NH (**II**) and N–NH_2 (**III**) plane, respectively. [b] This work; calculated for model systems **Ĩa**–**IĨIa**. [c] Calculated by Deeth et al. in ref 36. [d] Calculated for the model system of Mo; measured for the analogous W compound.

Table 9. Experimental (QCA-NCA) and Calculated Force Constants of Mo/W Complexes

	f_{NN}[a]		f_{MN}[a]		f_{MNN}[a]	
complex	QCA-NCA[b]	B3LYP[c]	QCA-NCA[b]	B3LYP[c]	QCA-NCA[b]	B3LYP[c]
$[W(N_2)_2(dppe)_2]$ (**Ib**)	16.43	16.28	2.66	2.93	0.70	~0.50
$[Mo(N_2)_2(PH_3)_4]$ (**Ia**)	–	16.72	–	2.41	–	~0.45
$[MF(NNH)(dppe)_2]$ (**II**)[e]	8.27	9.48	(~4.5)	5.29	0.53 (ip)	0.54 (ip)
$[MF(NNH_2)(dppe)_2]^+$ (**III**)[e]	7.20[d]	7.81	6.31	6.20	0.39 (oop) 0.69 (ip)	0.56 (oop) 0.40 (ip)

[a] Units are mdyn/Å for stretching and mdyn·Å for bending force constants. [b] See Part I of this series; abbreviations: ip and oop are in-plane and out-of-plane bends relative to the M–N–NH (**II**) and N–NH_2 (**III**) plane, respectively. [c] This work; calculated for model systems **Ĩa**–**IĨIa**. [d] Compare with $f_{NN} = 7.73$ for coordinated *trans*-diazene.[17] [e] Calculated for the model system of Mo; the experimental value was obtained for the analogous W compound.

occurs yielding the NNH_3 species which—in addition to the double π bond—is also σ bound to the metal.[21] Simultaneously, the remaining (vertical) N–N π bond of the NNH_2 intermediate is removed. Thus, the N–N bond has been transformed into a single bond whereas a triple bond is present between the metal and the coordinating nitrogen atom. This is exactly inverse to the situation in the parent dinitrogen complex.

To conclude, the reduction and protonation of N_2 along the asymmetric pathway by Mo/W systems is characterized by the following three factors:

(1) The parent dinitrogen complexes feature a moderately activated N_2 group with a charge of approximately −0.1 on the β-nitrogen.

(2) By each protonation step, covalency between the metal and the NNH_x unit is increased with the major change occurring after the first protonation. As a consequence, the resulting intermediate is stabilized, the relatively weak M–N bond of the dinitrogen systems is strengthened and the loss of charge due to addition of the proton is at least compensated. Negative charges on the intermediates below −1 are avoided.

(3) The N–N bond order is reduced by each step initiating N–N cleavage, and the terminal nitrogen atom of the intermediates NNH and NNH_2 is always negatively charged to enable further protonation.

On the basis of the second factor, the Mo and W systems successfully mediate these reactions *although the activation of the parent dinitrogen ligand is only moderate.* From a more general viewpoint, the role of covalency becomes less important if more charge is put on this ligand in the parent complex, i.e. if the degree of activation is increased. This can be achieved through coordination of N_2 to metals of lower effective nuclear charge Z_{eff} than Mo and W lying on the left-hand side of the transition-metal series. As a consequence, however, this also requires the use of stronger reductants to generate the dinitrogen complex which conflicts with the initially stated goal of "mild conditions". On the other hand, coordination to metals on the right-hand side of Mo and W (i.e. with a higher Z_{eff}) would act to weaken the activation of coordinated N_2 and also decrease the charge transfer to the partly reduced species. In nitrogenase, the bonding of N_2 to the multimetallic FeMo cofactor supposedly provides a much more efficient charge transfer to this ligand than attainable by monometallic centers. This enables nitrogen fixation at much less negative reduction potentials than in the synthetic systems considered here.

Comparison to Symmetric Reduction Pathway. Although not relevant to nitrogenase, transition-metal complexes with end-on bridging N_2 have repeatedly been considered in connection with synthetic nitrogen fixation.[16,39] Nevertheless, it appears that a significantly higher degree of activation is necessary for their reduction and protonation than for the end-on terminally coordinated systems investigated here. For example, binuclear dinitrogen-bridged tungsten systems only give moderate amounts of hydrazine and no ammonia[40] while their mononuclear counterparts produce high amounts of NH_3 (see above). In order to understand these differences in reactivity, a linear binuclear M1–N–N–M2 unit (M1, M2 = Mo/W) with moderately activated dinitrogen is considered (Scheme 1a). If one proton is added to the bridging N_2, a M1–N(H)–N–M2 structure results which is bent at, e.g., M1 (Scheme 1b). This breaks the in-plane π bond between M1 and N_2. Since π_h^* can only interact with an empty d_{z^2} orbital of M1 in a σ donor manner, one electron has to be transfered from the t_{2g}^* functions of M1 to π_h^*, equivalent with a one-electron oxidation of this metal and a concomitant reduction of the ligand. The addition of a second proton leads to the symmetric diazene species M1–N(H)–N(H)–M2 and rotates M2 out of the linear M–N–N

(39) (a) Collman, J. P.; Hutchison, J. E.; Lopez, M. A.; Guilard, R.; Reed, R. A. *J. Am. Chem. Soc.* **1991**, *113*, 2794. (b) Collman, J. P.; Hutchison, J. E.; Lopez, M. A.; Guilard, R. *J. Am. Chem. Soc.* **1992**, *114*, 8066. (c) Collman, J. P.; Hutchison, J. E.; Ennis, M. S.; Lopez, M. A.; Guilard, R. *J. Am. Chem. Soc.* **1992**, *114*, 8074.

(40) Anderson, S. N.; Richards, R. L.; Hughes, D. L. *J. Chem. Soc., Dalton Trans.* **1986**, 245.

Scheme 1

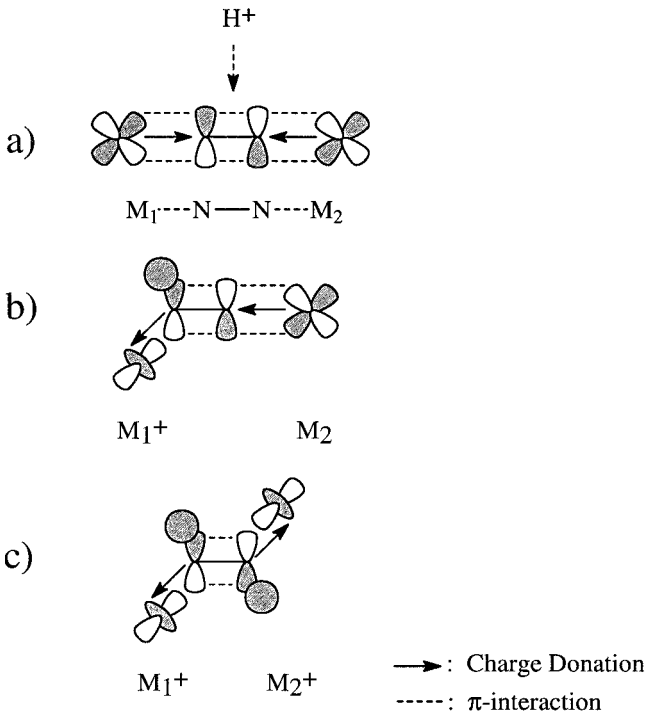

structure as well thus breaking the π bond between M2 and N_2 (Scheme 1c). In order to bind this species in a σ donor manner to both metal centers, the transfer of a second electron to π_h^*, this time from M2, is necessary. Thus, at the stage of diazene two π bonds have been broken and two σ bonds have been formed; both metal centers have been one-electron oxidized, the ligand has been two-electron reduced and two geometrical rearrangements have occurred. Moreover, the double protonation of μ-1,2 diazene leading to hydrazine again requires two one-electron oxidations of both metal centers and disrupts the remaining out-of-plane metal−N π bonds.[17] This way, two M−N σ donor and π acceptor bonds are replaced by two weaker σ single bonds which is thermodynamically unfavorable.[17] Further protonation of N_2H_4 requires another rearrangement to an end-on terminal configuration, i.e. one metal−N bond of the bridging M−N(H_2)−N(H_2)−M structure must be broken which again is endothermic (cf. ref 41). In addition, there is some probability that hydrazine is lost at this stage.

On the basis of these mechanistic drawbacks, the symmetric reduction pathway involving μ-1,2 N_2, N_2H_2, and N_2H_4 species appears less favorable for the reduction and protonation of coordinated dinitrogen in small-molecule systems. Whereas the asymmetric pathway allows a gradual flow of electron density from the metal to the protonated ligand with a smooth conversion from π backbonding to a π double bond, the corresponding protonation steps of the symmetric pathway are accompanied by much larger changes of geometry and redistributions of electron density which raise the activation barriers to these reactions. Furthermore, while in case of the asymmetric pathway every protonation leads to a strengthening of the M−N bond fixing the partly reduced intermediate tighter to the metal, the metal−N bond strength is *reduced* again after the diazene stage in the symmetric pathway, leading to weakly bound hydrazine. All of these differences can be traced back to the fact that in the asymmetric reduction pathway the bonding and the protonation site of the coordinated dinitrogen are separated whereas these two functions are performed at the same site in the symmetric pathway. In summary, therefore, the asymmetric pathway appears as the more effective reduction mode of dinitrogen.

Acknowledgment. F.T. gratefully acknowledges the support of these investigations by the Deutsche Forschungsgemeinschaft (Grant Tu58/5-1) and Fonds der Chemischen Industrie (FCI) and thanks Dr. R. L. Richards, Nitrogen Fixation Laboratory, John Innes Center, Norwich (U.K.) for a sample of [W(N_2)$_2$-(depe)$_2$]. Preparative work of N. Böres is gratefully acknowledged. N.L. thanks FCI for a Kekulé Research Fellowship. We thank the Emil und Paul Müller Gedächtnisstiftung, Universität Mainz, for financial aid.

IC9809409

(41) Demadis, K. D.; Malinak, S. M.; Coucouvanis, D. *Inorg. Chem.* **1996**, *35*, 4038.